Morphogen gradient formation in a complex environment: An anomalous diffusion model

Gil Hornung,[1] Brian Berkowitz,[1,*] and Naama Barkai[2]
[1]*Department of Environmental Sciences and Energy Research, Weizmann Institute of Science, Rehovot, 76100 Israel*
[2]*Department of Molecular Genetics and Department of Physics of Complex Systems, Weizmann Institute of Science, Rehovot, 76100 Israel*

(Received 31 March 2005; revised manuscript received 21 June 2005; published 17 October 2005)

Current models of morphogen-induced patterning assume that morphogens undergo normal, or Fickian, diffusion, although the validity of this assumption has never been examined. Here we argue that the interaction of morphogens with the complex extracellular surrounding may lead to anomalous diffusion. We present a phenomenological model that captures this interaction, and derive the properties of the morphogen profile under conditions of anomalous (non-Fickian) diffusion. In this context we consider the continuous time random walk formalism and extend its application to account for degradation of morphogen particles. We show that within the anomalous diffusion model, morphogen profiles are fundamentally distinct from the corresponding Fickian profiles. Differences were found in several key aspects, including the role of degradation in determining the profile, the rate by which it spreads in time and its long-term behavior. We analyze the effect of an abrupt change in the extracellular environment on the concentration profiles. Furthermore, we discuss the robustness of the morphogen distribution to fluctuations in morphogen production rate, and describe a feedback mechanism that can buffer such fluctuations. Our study also provides rigorous criteria to distinguish experimentally between Fickian and anomalous modes of morphogen transport.

DOI: 10.1103/PhysRevE.72.041916 PACS number(s): 87.18.La, 05.40.−a, 82.39.−k, 46.65.+g

I. INTRODUCTION

Multicellular organisms develop through the specification of particular tissue types in well defined spatial positions. Often, such patterning is mediated by signaling molecules, termed morphogens, which can induce several cell fates in a concentration-dependent manner. Morphogens are produced at localized sites, and spread into the tissue to define a long-range concentration gradient. Cells across the tissue undertake a specific cell fate according to the morphogen level at their position. Molecules that function as morphogens in a wide range of organisms include the Bone-morphogenesis protein (BMP/Dpp/Nodal), the Hedgehog (Hh), and the Wingless (Wg/Wnt) families (reviewed in Refs. [1,2]).

Understanding how morphogen gradients are established and maintained is a central issue in developmental patterning. Morphogens move within the extracellular milieu that is densely packed with proteins that belong to a family called heparan sulfate proteoglycans (HSPG). Recent studies demonstrated that the interaction of morphogens with HSPG plays a crucial role in defining the morphogen profile (recently in Refs. [3–8] and reviewed in Refs. [1,9]). HSPG proteins reside on the cell surface and are linked to saccharide chains that undergo a variety of modifications and form binding sites for morphogens [9]. Important features of the HSPG and their saccharide chains are their high degree of molecular heterogeneity and the disordered structures they form. It has been suggested that HSPG can facilitate morphogen movement through several mechanisms, including diffusion through HSPG binding sites [5], movement of the saccharide chains or the entire HSPG together with the bound morphogens [5,9], or active transport that includes cellular uptake and secretion of morphogens (transcytosis) [10,11].

All current models assume that morphogen movement in the extracellular environment is described by Fickian, i.e., "normal," diffusion, and can thus be modeled using a conventional reaction-diffusion formalism (e.g., Refs. [11–14]). Underlying this notion is the assumption that morphogens move via a series of random transitions, which are characterized by a well-defined length scale and a finite mean transition time. However, this Fickian assumption often does not hold for transport phenomena in disordered, microscopically heterogeneous structures. Indeed, experiments in diverse systems, including carrier transport in amorphous materials [15,16], diffusion in polymers [17–19], turbulent systems [20], and flow through porous media [21,22] identified anomalous, rather than Fickian, transport. Moreover, movement of proteins on cell membranes (reviewed in Refs. [23,24]) and inside cells (for example, Refs. [25–27]) has been shown to accord with anomalous transport. In such cases continuous time random walk (CTRW) theory [28–30] offers a viable framework to quantify this behavior.

In this study we use the CTRW formalism to describe the possible impact of anomalous diffusion on morphogen distribution, extending the theory to include morphogen particle degradation. We show that the anomalous diffusion profile converges rapidly to an exponential shape, whose amplitude and length scale increase with time. For potentially long periods of time the anomalous diffusion profile is insensitive to degradation, but depends on parameters describing the interaction with the extracellular environment. Unlike in Fickian diffusion, the morphogen profile does not approach a steady state but continues to evolve in time, albeit at a vanishingly slow rate. We discuss the capacity of the anomalous profile to buffer fluctuations in morphogen production rate, and de-

*Electronic address: brian.berkowitz@weizmann.ac.il

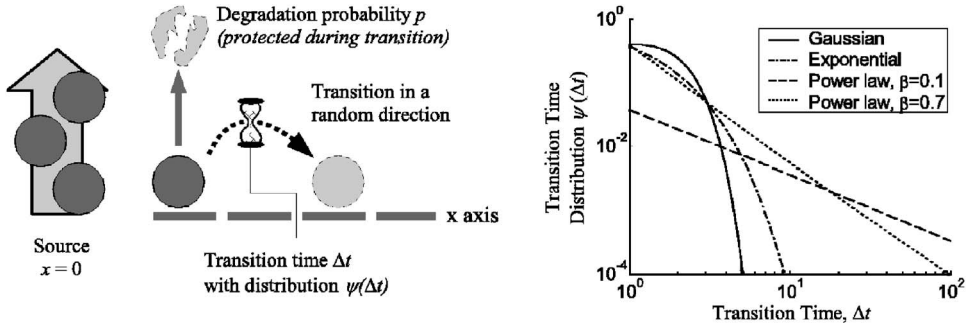

FIG. 1. Random walk model for anomalous diffusion. (a) Scheme of suggested random walk model: A morphogen is released from a source and performs transitions of a random distance and direction along the x axis. The time required to complete a transition Δt is a random variable from a distribution $\psi(\Delta t)$. At the start (or end) of each transition the morphogen can be degraded with a probability p. (b) Possible forms of transition time distributions. Shown are Gaussian and exponential distributions (mean and standard deviation equal to 1) and power law distributions (Eq. (1), $\tau=1$).

scribe a feedback mechanism that ensures this robustness. Finally, we derive rigorous criteria to distinguish experimentally between Fickian and anomalous transport.

II. THEORY AND ANALYSIS

A. Random walk model for morphogen diffusion

Morphogen movement can be described using the following random walk formalism [Fig. 1(a)]. We assume that morphogen molecules are produced continuously in a one-dimensional domain at some fixed position ($x=0$) and move by a series of hops, referred to as "transitions." The duration of each such transition is Δt, and its distance is Δx, in a random direction; Δx is much smaller than the order of the cell size. After a morphogen molecule completes a transition, it can be degraded with some probability p, or perform another hop with the probability $1-p$. Hence, morphogen degradation occurs only at the end of a transition, and the morphogen is protected during the time of the transition itself.

This random walk model is a generic model for diffusion with degradation. Physically, the surrounding in which the morphogen moves determines the distributions of the transition times and the transition lengths, which we denote by $\psi(\Delta t)$ and $f(\Delta x)$, respectively. Morphogen entrapment within HSPG could enter this scheme by leading to long transition times. To account for this we consider a power law form for the transition time distribution

$$\psi(\Delta t) \sim \frac{1}{\tau}\left(\frac{\Delta t}{\tau}\right)^{-1-\beta}, \tag{1}$$

where τ is some constant with dimension of time. Indeed, this distribution decays slowly for long transition times [compared, for example, to Gaussian or exponential forms, Fig. 1(b)], and the power law exponent, β, controls the prominence of long transition times [Fig. 1(b)]. When $\beta<1$, long transition times become so dominant that the mean transition time is, in fact, infinite. Phenomenologically, β quantifies the degree of interaction between HSPG and morphogens, and serves as a criterion to differentiate between anomalous and Fickian diffusion [Fig. 2(a)]: When $\beta>1$ the probability to encounter high transition times is negligible and the diffusion is Fickian, but for $\beta<1$ high transition times are prominent and the diffusion is anomalous (for a more rigorous discussion of this behavior see Ref. [31]).

B. Analytical derivations using CTRW

To obtain analytical expressions from the random walk model we use the CTRW formalism. The CTRW framework relates the morphogen concentration profiles to the two aforementioned distributions $\psi(\Delta t)$ and $f(\Delta x)$. To account for degradation of morphogen particles we extend the CTRW formalism through the inclusion of a degradation time distribution $\phi(\Delta t)$ [32]. Degradation and movement are assumed to be mutually exclusive, hence, for example, degradation can occur only after the completion of a transition. From this condition the transition time distribution normalizes to $1-p$ and the degradation time distribution normalizes to p [32]

$$p = \int_0^\infty \phi(t)dt = 1 - \int_0^\infty \psi(t)dt.$$

Note that if we were to assume an alternative case, in which degradation is independent of transitions and has a constant rate, then long transition times will be eliminated and anomalous behavior will not prevail (not shown here).

We first analyze the spatial distribution of morphogens due to a unit pulse of morphogens (also termed the Green's function), $C_G(x,t)$, and only then introduce continuous morphogen production. $C_G(x,t)$ is equivalent to the probability of finding a morphogen at position x at time t, and it can be expressed by

$$C_G(x,t) = \int_0^t \Pi(t-t')R(x,t')dt', \tag{2}$$

where $R(x,t)$ is the probability for a morphogen to "just arrive" at position x at time t, and $\Pi(t)$ is the probability of not leaving position x or being degraded during a time period of length t [32]:

$$\Pi(t) = 1 - \int_0^t \psi(t')dt' - \int_0^t \phi(t')dt'. \tag{3}$$

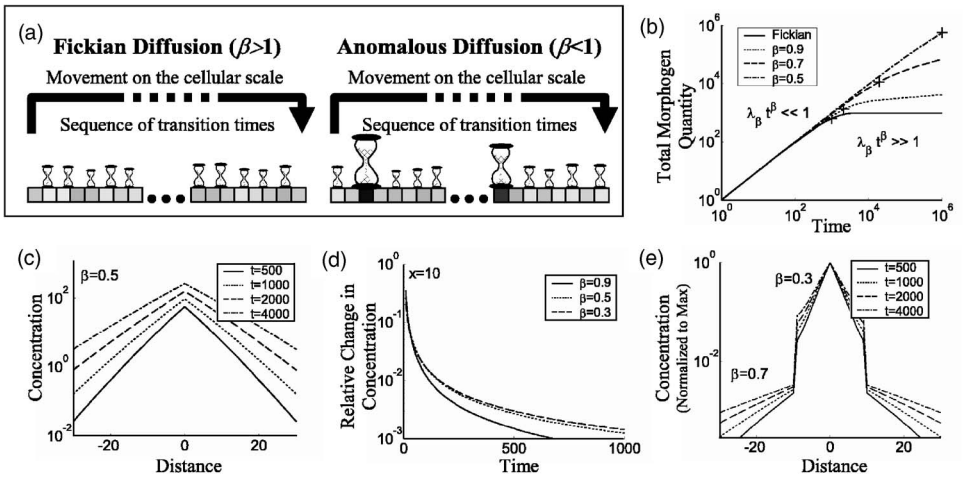

FIG. 2. Causes and effects of anomalous diffusion. (a) A morphogen particle undergoing diffusion encounters a large number of transition events with various transition times represented by hourglass sizes. Over distances on the order of the cellular scale the diffusion becomes Fickian (left) if there is a narrow distribution of transition times, and anomalous if the distribution is broad and allows very high transition times (right). The parameter β that is defined in Eq. (1) separates between the two cases. (b) Total number of morphogens vs. time for Fickian diffusion and various values of β. Crosses point at time $t_{\mathrm{deg}}=\lambda_{\beta}^{-1/\beta}$, near which the transition between the early and late time regimes occurs. (c) The concentration profile at the early time regime. Plotted for $\beta=0.5$ and for various times appearing in the legend. (d) The relative rate of change in concentration, $(1/C)(\partial C/\partial t)$, at a specific position was plotted for various values of β appearing in the legend. The plot is for $x=10$, but similar behavior is obtained for other positions. (e) Modeling the effect of clones via a sharp change of β. The values of β are $\beta=0.3$ and $\beta=0.7$ in the ranges $|x|<10$ and $|x|>10$, respectively. Degradation is assumed to be negligible. Plots are the result of a numerical inverse Laplace transform [56] of Eqs. (47a) and (47b) in Sec. V of Ref. [57]. Concentration is normalized to the maximum concentration. Unless otherwise mentioned all plots were generated by performing a numerical inverse Laplace [56] of Eqs. (13) or (10) derived in Sec. II. Parameter values are $\lambda=\lambda_{\beta}=0.001$, $J_0=1$, and $D=D_{\beta}=1$.

Using standard CTRW methods [28–30] the Fourier-Laplace transform of $R(x,t)$ can be expressed by

$$\hat{\tilde{R}}(k,u)=\frac{1}{1-\hat{f}(k)\tilde{\psi}(u)}, \tag{4}$$

where k is the Fourier variable replacing distance and u is the Laplace variable replacing time. The hat and the tilde denote Fourier and Laplace transformed functions, respectively. Substituting Eq. (4) and the Laplace transform of Eq. (3) into the Fourier-Laplace transform of Eq. (2) we find

$$\hat{\tilde{C}}_G(k,u)=\frac{1-\tilde{\psi}(u)-\tilde{\phi}(u)}{u}\frac{1}{1-\hat{f}(k)\tilde{\psi}(u)}. \tag{5}$$

A constant influx of morphogens entering at $x=0$ can be viewed as the integration over time of a pulse input

$$C(x,t)=J_0\int_0^t C_G(x,t')dt', \tag{6}$$

where J_0 is the morphogen production rate in units of morphogen quantity per area per time. From Eqs. (5) and (6) we obtain

$$\hat{\tilde{C}}(k,u)=J_0\frac{1-\tilde{\psi}(u)-\tilde{\phi}(u)}{u^2}\frac{1}{1-\hat{f}(k)\tilde{\psi}(u)}. \tag{7}$$

Equation (7) is a general expression for the concentration profile of a system with degradation and constant production, and can be used with any form of the transition and degradation distributions.

We now introduce asymptotic forms for $\psi(\Delta t)$, $\phi(\Delta t)$, and $f(\Delta x)$. We assume that degradation is instantaneous

$$\phi(\Delta t)=p\,\delta(\Delta t). \tag{8}$$

We consider a transition time distribution that has a power law tail with an exponent $\beta<1$ [Eq. (1)]. The transition lengths are assumed to be distributed with a mean of zero (unbiased walk) and a finite variance l^2. We are interested in the concentration profile over distances that are much larger than the scale of single transitions, $x\gg l$, and in times that are $t\gg\tau$. Under these conditions $\psi(\Delta t)$ and $f(\Delta x)$ are approximated by (see Sec. I of Ref. [57] for derivation)

$$\tilde{\psi}(u)\approx(1-p)[1-(\tau u)^{\beta}], \tag{9a}$$

$$\hat{f}(k)\approx 1-\frac{l^2}{2}k^2, \tag{9b}$$

and

$$\hat{f}(k)\tilde{\psi}(u)\approx(1-p)\left(1-(\tau u)^{\beta}-\frac{l^2}{2}k^2\right). \tag{9c}$$

The approximation in Eq. (9a) is valid only for $0<\beta<1$.

As mentioned before, we assume that degradation is instantaneous and is given by Eq. (8). Substituting Eqs. (9a)–(9c) and (8), into Eq. (7), and taking the inverse Fourier transform, we obtain for small p

$$\tilde{C}(x,u) = \frac{J_0}{2}\frac{\exp(-m|x|)}{D_\beta m u^{2-\beta}}, \tag{10}$$

where

$$m = D_\beta^{-1/2}\sqrt{\lambda_\beta + u^\beta}, \tag{11}$$

with $D_\beta = l^2/2\tau^\beta$ and $\lambda_\beta = p/\tau^\beta$. A similar function for $C(x,t)$ was obtained from a different method based on the Montroll-Weiss equation (see Sec. II of Ref. [57] for derivation).

The total number of morphogens in the system $S(t)$ is found by taking $k=0$ in Eq. (7), which is equivalent to integrating the concentration over the entire space

$$\tilde{S}(u) = J_0\frac{1-\tilde{\psi}(u)-\tilde{\phi}(u)}{u^2}\frac{1}{1-\tilde{\psi}(u)}. \tag{12}$$

In Section III of Ref. [57] we rederive Eq. (12) independently of the spatial diffusion component. Upon substitution of functional forms in Eqs. (9a)–(9c) and (8), into Eq. (12) we obtain

$$\tilde{S}(u) = \frac{J_0}{u^{2-\beta}(\lambda_\beta + u^\beta)}. \tag{13}$$

To complete the solution, we derived analytical approximations for the inverse Laplace transform of Eqs. (10) and (13) (Sec. IV of Ref. [57]).

C. Simulations

All results derived by CTRW were verified using direct numerical simulations of the random walk model. Morphogen diffusion is simulated by a series of discrete transition events. The transition time is represented as the time a morphogen waits before moving. When the duration of the transition time ends, the morphogen can either move with probability $1-p$ or degrade with probability p. Movement is implemented by adding a pseudorandom number to the position of the morphogens, sampled from the Gaussian distribution with mean zero and variance l^2. After each movement a new transition time is generated from a power law distribution that accords with Eq. (1):

$$\psi_{\mathrm{PL}}(\Delta t) = \frac{\beta}{h_{\mathrm{PL}}\tau}\left(\frac{\Delta t}{h_{\mathrm{PL}}\tau}+1\right)^{-1-\beta}, \tag{14}$$

where $h_{\mathrm{PL}} \equiv \Gamma(1-\beta)^{-1/\beta}$. The value of h_{PL} is set such that the Laplace transform of $\psi_{\mathrm{PL}}(\Delta t)$ and the transition time distribution used in the analytical derivation [Eq. (9a) with $p=0$] have the same asymptotic ($u\to 0$) functional form. At any given time step the concentration profile is deduced from the histogram of the morphogen positions.

To reduce computation time we simulate concentration profiles that result from a pulse input of morphogens, and then numerically integrate the results over time to obtain the response to a constant production of morphogens. This method can be utilized only when morphogen transitions are independent of each other and of time. To simulate recovery experiments and feedback scenarios we add particles at every time step instead of performing the integration.

III. RESULTS

In the next sections we describe the properties of concentration profiles that are generated if HSPG trap diffusing morphogens for long periods of time, leading to anomalous transport [Fig. 2(a)]. We compare these profiles to profiles generated by a Fickian diffusion process. We then focus on the system from a biological perspective, by analyzing the effect of mutants and macroscopic heterogeneities in HSPG, by studying the robustness of the morphogen gradients to fluctuations and by suggesting experimental methods for validating the anomalous behavior.

A. Parameters controlling morphogen profile under conditions of anomalous diffusion

A major difference between a random walk model under Fickian assumptions and a random walk model with a broad transition time distribution is apparent in the number of molecular transitions of an average morphogen particle, $\langle n\rangle_{(t)}$. When the diffusion is Fickian, $\langle n\rangle_{(t)}$ is proportional to time, and the parameters that control the morphogen distribution are the three parameters of the reaction-diffusion equation: the morphogen production rate J_0, the degradation rate λ and the diffusion coefficient D.

However, when long transition times dominate, the average number of transitions increases as a power law with time

$$\langle n\rangle_{(t)} \propto \left(\frac{t}{\tau}\right)^\beta, \tag{15}$$

where τ is some time constant, and the value of β, that signifies the interactions with the HSPG, is smaller than one. This scaling law changes the behavior of the morphogen distribution and rescales the diffusion and degradation coefficients. The length scale of the concentration profile becomes $\sqrt{D_\beta t^\beta}$ (Appendix A), with a generalized diffusion coefficient [33] D_β given in dimensions of length per time to the power of β. In addition, the time t_{deg} at which degradation begins to play a role in shaping the profile is given by $\lambda_\beta t_{\mathrm{deg}}^\beta = 1$ (Appendix A), with a degradation coefficient λ_β in dimensions of time to the power of $-\beta$ (see Sec. II B for exact definitions of D_β and λ_β). Notably, as β approaches one, the parameters controlling Fickian and anomalous parameters become identical.

B. Time-dependent morphogen profile under conditions of anomalous diffusion

Using the CTRW framework, we find a rigorous solution of the morphogen concentration profile as a function of time (Sec. IV of Ref. [57]). We identify two time regimes of the solution [Table I, Fig. 2(b)]. At early times, when $\lambda_\beta t^\beta \ll 1$, degradation is negligible and morphogen quantity rises linearly with time. The shape of the morphogen profile at the early time regime converges rapidly to an exponential [Fig. 2(c) and Table I], with both its amplitude and spread increasing as a power law with time. The exponent of this power law is related to $\beta/2$ (Table I). Hence in the early time regime HSPG properties, as captured by β, set the profile rather than degradation.

TABLE I. Expressions for morphogen profile and total morphogen quantity, for the reaction-diffusion model (Fickian diffusion) and anomalous diffusion model. J_0 is the morphogen production rate in units of morphogen quantity per time per area, D is the diffusion coefficient, D_β is its analog for anomalous diffusion, λ is the degradation rate and λ_β is its anomalous diffusion counterpart. The expressions for anomalous diffusion are first-order approximations. For more elaborate expressions and derivation see Sec. IV of Ref. [57].

	Anomalous diffusion		Reaction diffusion (Fickian)	
	Early time regime $\lambda_\beta t^\beta \ll 1$	Late time regime $\lambda_\beta t^\beta \gg 1$	Presteady state $\lambda t \ll 1$	Steady state $\lambda t \gg 1$
Profile shape	Exponential $A(t)e^{-\alpha(t)x}$	Exponential $A(t)e^{-\alpha x}$	Gaussian profile to exponential	Exponential $Ae^{-\alpha x}$
Profile amplitude $A(t)$	$\frac{J_0}{2\sqrt{D_\beta}}t^{1-\beta/2}$	$\frac{J_0}{2\sqrt{\lambda_\beta D_\beta}}t^{1-\beta}$		$\frac{J_0}{2\sqrt{\lambda D}}$
Profile inverse length scale $\alpha(t)$	$\frac{1}{\sqrt{D_\beta}}t^{-\beta/2}$	$\sqrt{\lambda_\beta/D_\beta}$		$\sqrt{\lambda/D}$
Total morphogen per unit area	$J_0 t$	$\frac{J_0}{\lambda_\beta}t^{1-\beta}$	$\frac{J_0}{\lambda}(1-e^{-\lambda t})$	J_0/λ

Conversely, at late times, when $\lambda_\beta t^\beta \gg 1$, degradation plays an important role in shaping the morphogen distribution (Table I). Interestingly, at those late times, the total number of morphogens continues to rise [Fig. 2(b) and Table I]. Thus, in contrast to the case of Fickian diffusion, the anomalous diffusion profile does not reach a steady state, and its amplitude continues to grow in time (Table I). Also, the Fickian diffusion profile assumes an exponential shape only at the steady state, whereas the anomalous diffusion profile reaches an exponential shape already at the early time regime [Table I and Fig. 2(c)].

A consequence of this analysis is that morphogen concentration profiles depend on time. However the rate at which they evolve becomes vanishingly small with time, and will in practical terms appear to be stable [Fig. 2(d)].

As we discuss below, morphogen degradation may be subject to genetic or environmental fluctuations. The early time regime, being degradation independent, is responsive to fewer types of fluctuations and is thus more advantageous than the late time regime, which is degradation dependent. Moreover, the anomalous diffusion at the early time regime is more robust to degradation than is the reaction-diffusion model at steady state, which also depends on degradation (Table I). Therefore, in the following we focus the discussion on the early time regime.

C. Gradients with a sharp change in β show a time-dependent discontinuity

The analysis above considered morphogens that move in a field with a constant β, corresponding to a uniform distribution of HSPG across the tissue. Yet, a common experimental practice to study HSPG is through generation of clones of HSPG mutant cells within the wild type tissue (e.g., Refs. [4,6,34]). To facilitate the understanding of such studies in the situation of anomalous diffusion, we consider mutated HSPG clones characterized by a β value that is distinct from that found elsewhere in the field, and study the behavior at the clone boundary (Appendix B).

When β changes abruptly in space, morphogens accumulate at the region with the lower β, leading to a time-dependent discontinuity of the profile at the clone boundary [Fig. 2(e)]. We find that the ratio of the morphogen concentrations on the two sides of the clone boundary increases as a power law (Appendix B and Sec. V of Ref. [57]):

$$\frac{C_1(x_{\text{th}},t)}{C_2(x_{\text{th}},t)} \approx t^{\beta_2-\beta_1}, \tag{16}$$

where C_1 and C_2 denote concentrations closer and further from the source, respectively, and x_{th} is the position of the boundary. Also, far from the clone boundary $C_2(x,t)$ assumes the same slope as the anomalous profile described above (Table I), with a constant $\beta=\beta_2$.

D. Robustness to morphogen production rate

To ensure reliable developmental patterning, morphogen gradients need to be buffered against environmental and genetic fluctuations. Because morphogens are produced only in a specific position, but they spread throughout the tissue, buffering fluctuations of the morphogen production rate is particularly important. We have shown recently that the sensitivity of the profile to the production rate depends on the slope of the morphogen profile close to its source [12]. In the present case of anomalous diffusion this slope is controlled by β. Indeed, the shift in the profile following a change in production rate is significantly more pronounced for high β than for low β [Figs. 3(a) and 3(b)]. Yet, lowering β also reduces the spatial range of the morphogen [Fig. 3(a)]. In

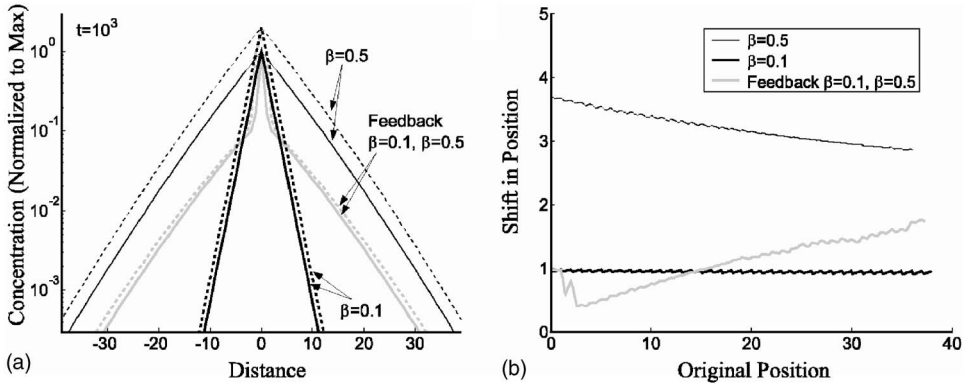

FIG. 3. Robustness to morphogen production rate. (a) Effect of doubling morphogen production rate on the concentration profile. Solid lines are unperturbed concentration profiles, and dotted lines represent the effect of doubling production rates. Black bold and black thin lines are morphogen profiles without feedback for $\beta=0.1$ and $\beta=0.5$, respectively. Shown in gray are feedback simulation results (Sec. II C; Sec. VI of Ref. [57]) with $\beta=0.1$ above a threshold concentration and $\beta=0.5$ below it. The threshold value is 50 morphogens per unit area. The plots for each value of β are normalized to the maximal concentration. Original production rate is 1 morphogen per time unit. Concentrations shown in the figure are for $t=1000$, with 3×10^6 morphogen particles in the system (3000 morphogens were added per time step). Results are an average of 45 simulations. The bin size used in the simulations to calculate morphogen concentrations from the histogram of the morphogen positions was 1/64 length units (see Sec. VI of Ref. [57] for simulation details). (b) The shift in the position of cells responding to a certain concentration, when morphogen production rate is doubled. The shift is plotted against the original position of the cells, and is a measure of the robustness—small shifts signify systems that are robust to morphogen production rate.

fact, this opposing interplay between the capacity to buffer fluctuations and the spatial morphogen range is inherent to exponential profiles which are characterized by a single decay length [12].

A possible way to break the interplay between robustness and spatial range is to introduce a feedback that enhances the decay of the profile close to the source [12]. In the case of Fickian diffusion this can be achieved through enhancement of morphogen degradation in a morphogen-dependent manner [12], but because the anomalous diffusion profile does not depend on degradation we consider an alternative feedback which reduces β near the source. Indeed, an effect of morphogen signaling on HSPG was observed, either via modulation of some HSPG property, e.g., induction of an HSPG-modifying enzyme [7,8,35–38], or by changing the level of the HSPG themselves [34,39]. To study such a feedback mechanism, we simulate a system where β depends on the morphogen level (for simulation details see Sec. II herein and Sec. VI of Ref. [57]). Specifically, we assume that $\beta=\beta_1$ in regions where morphogen levels are above some threshold, while in regions of lower morphogen levels β assumes a higher value $\beta_2>\beta_1$. We note that this situation differs from the case of a clone discussed above, because here the spatial boundary between the regions of differential β are co-established with the concentration itself, rather than being left unchanged throughout the build-up of the concentration profile.

Simulation results demonstrate that such feedback indeed enhances buffering capacity, while still allowing morphogens to reach a wide spatial range [Figs. 3(a) and 3(b)]. In fact, the sensitivity of the system to perturbations in morphogen production rate is defined by the low value $\beta=\beta_1$, while its spatial range is defined to a good approximation by the higher value β_2 [Figs. 3(a) and 3(b)]. Thus, a feedback that alters HSPG properties and defines lower β values in a region of high morphogen level breaks the interplay between robustness and spatial range and provides a general means for enhancing the capacity to buffer fluctuations in morphogen production rate.

E. Toward experimental verification of anomalous diffusion

Our analysis above shows that under conditions of anomalous diffusion, the behavior of the morphogen distributions differs considerably from the case of the commonly assumed Fickian diffusion. These results reinforce the need to examine whether in actual systems morphogen diffusion is Fickian or anomalous. Some information could, in theory, be gathered from visualization of the concentration profile using GFP fusion or direct antibody staining (e.g., Refs. [7,10,40,41]). However, such methods are compromised by the difficulties in obtaining precise quantitative descriptions of the morphogen levels over long times, and the fact that quantitative values of the diffusion or degradation parameters are not available. We therefore consider an alternative means to distinguish experimentally between the anomalous and the Fickian diffusion situations.

Fluorescent recovery after photobleaching (FRAP) is a common approach to analyze diffusion properties. In this method, the diffusing protein is tagged by a fluorescent marker, and in the course of the experiment the fluorescence is removed in a well-defined region via photobleaching. Measurement of the temporal recovery of fluorescence inside the bleached region can then be used to extract quantitative information on the diffusion [42–44]. FRAP has been used in the past to characterize anomalous diffusion on the level of a single cell (e.g., Refs. [45,46]), and we suggest to extend it to the tissue scale.

To examine whether FRAP experiments can be used to distinguish between Fickian and anomalous diffusion in mor-

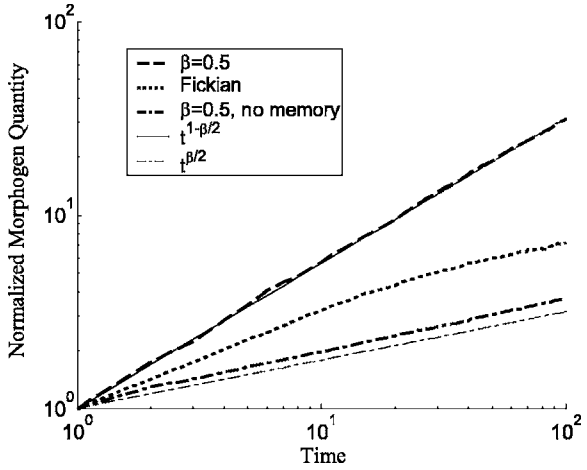

FIG. 4. FRAP simulations. Recovery is shown on log-log scales, such that the slopes of the curves represent the power law exponents. Recovery under condition of anomalous diffusion ($\beta=0.5$, dashed line) rises with a power law exponent $1-\beta/2$. Fickian diffusion (dotted line) rises with a power law exponent of 0.5 for short times. Simulations of anomalous diffusion in which the morphogen transition times were set to zero before the bleach (dash-dot) resulted in a power law exponent $\beta/2$. The bleached region was between $x=10$ and $x=20$. In simulations of anomalous diffusion the bleach time was 10^4 and in simulations of Fickian diffusion the bleach time was 10^3. The diffusion coefficients are $D_\beta=D=1$. Curves are normalized to the value at $t=1$.

phogen gradients, we simulate such an experiment. We find that in the case of anomalous diffusion, the intensity inside the bleached region increases as $t^{1-\beta/2}$ (Fig. 4), distinguishing it from Fickian diffusion, which rises as $t^{1/2}$ at short times [47]. The lower the value of β, the greater is the distinction between Fickian and anomalous behavior.

We note that our results differ from those of a previous analysis which predicted an increase of the form $t^{\beta/2}$ [48]. This previous work, however, neglected the fact that at the time of bleaching, a large fraction of morphogen molecules are at midtransition and cannot be made available immediately for diffusion (Appendix C). It is in fact the time-dependent release of those "trapped" morphogens that significantly enhances the observed recovery exponent. (A more analytical treatment of the problem using aging continuous time random walks [49] is considered in Appendix C and in Sec. VII of Ref. [57]). We thus suggest that FRAP experiments can indeed be used to determine whether morphogen diffusion in the presence of HSPG is described by Fickian or anomalous diffusion.

IV. DISCUSSION

To precisely understand the impact of HSPG on shaping morphogen gradients, a detailed description of the molecular interactions between morphogens and HSPG is required. While such data are not yet available, phenomenological analysis can still be used to distinguish between different qualitative effects of such an interaction. In particular, all models of morphogen movement can be described mathematically by a unified random walk formulation, whose qualitative features are determined completely by the distributions of the transition lengths and times.

Previous models of morphogen movement assume Fickian diffusion (e.g., Refs. [11–14]), implying that the transition times are distributed around a finite mean. Yet the diversity in HSPG structure and the multitude of their interactions with the morphogens suggest otherwise. In fact, an emerging notion, which is based largely on experiments in diverse systems, is that most natural processes that occur in complex environments are better described by transition time distributions with a power law tail, leading to anomalous rather than Fickian diffusion. To date the assumption of Fickian diffusion in morphogen systems has not been verified, and the possible impact of anomalous diffusion on morphogen distribution has not been examined.

This study provides a rigorous framework for analyzing morphogen profiles under conditions of anomalous diffusion. Our main assumption is that the interaction between HSPG and morphogens can be captured by the effective width of the transition time distribution, which we describe by a phenomenological parameter β. To study the effect of long tailed transition time distributions we utilize CTRW theory, and extend it to incorporate the first-order reaction of morphogen degradation. We show that for $\beta\rightarrow 1$ our model reduces to the reaction-diffusion equation, while for $\beta<1$ it allows long transition times corresponding to anomalous diffusion.

The model requires that morphogens have a constant probability for degradation per transition, rather than per unit time. This could occur, for example, if the morphogen moves by binding to a particular HSPG site and then hopping to an alternative site. The hop may either be successful, or may result in a loss of morphogen to the space away from the surface of the cells (the equivalent of degradation). This model is also compatible with the situation where binding to the HSPG protects the morphogen from enzymes that can degrade it. Indeed, the notion that HSPG are responsible for enhanced morphogen stability was suggested by several authors (e.g., Refs. [3,50]).

Our results demonstrate that anomalous diffusion drastically alters qualitative properties of morphogen distribution, and presents the system with unique challenges. At early times the anomalous morphogen profile is insensitive to morphogen degradation, but is controlled by interactions with HSPG. There is ambiguity in the literature on how important morphogen degradation is for shaping the profile. For example, Dpp degradation rate is faster than the rate of gradient build-up [41] implying that degradation is important. In contrast, the Wingless morphogen gradient formation rate is much faster [40], and is possibly on the order of magnitude of Wingless degradation. As such, degradation may not contribute to the build-up of the Wingless gradient.

If the impact of HSPG properties is greater than the impact of the degradation rates, modulation of HSPG by morphogens could serve as an important mechanism for controlling the properties of the morphogen profiles, as suggested by experimental observations (e.g., Refs. [7,8,34,37–39]). We showed that feedback on HSPG properties, which follows the principles of Ref. [12], induces robustness to fluctuations in the morphogen production rate.

Our analysis further revealed that when the field in which diffusion occurs is broken into two regions of disparate transition time distributions, then the concentration profile shows a time dependent discontinuity on the boundary between the two regions. This striking finding can have implications to the study of HSPG mutant clones inside a wild-type tissue.

Our model assumes diffusion in a one-dimensional domain. This is justified for situations such as development of the Drosophila wing imaginal disc, which has an approximate two-dimensional geometry with morphogen secreted from a linelike source. In other situations the geometry may be more complex, but the methodology introduced and the central qualitative results of our analysis are expected to be independent of geometry.

Whether morphogen diffusion is anomalous or Fickian remains an open question. Although some quantitative data on morphogen gradient formation exist in the literature [10,41], they are not at a high enough resolution to distinguish between the two types of diffusion. We suggest a rigorous experimental system, based on fluorescent recovery after photobleaching (FRAP), that can achieve this distinction. Interestingly, the fluorescent recovery of the morphogen system behaves differently than that predicted for systems containing newly synthesized particles [48]. In light of the likelihood of anomalous diffusion, further experimental work is undoubtedly required to gain insight into this critical issue.

ACKNOWLEDGMENTS

We thank Avigdor Eldar, Gennady Margolin and Harvey Scher for valuable discussions. This work was supported by the Sussman Family Center of Environmental Research (B.B.), the Israel Science Foundation, and the Minerva Foundation (N.B.).

APPENDIX A: SCALING CONSIDERATIONS IN ANOMALOUS DIFFUSION

Many of properties of anomalous diffusion can be explained by the scaling of the number of transitions that an average morphogen undergoes up to time t. When the diffusion is Fickian the average number of transitions is proportional to t/τ_m, where τ_m is the mean transition time. Conversely the average number of transition in anomalous diffusion is

$$\langle n\rangle_{(t)} \propto \left(\frac{t}{\tau}\right)^{\beta} \tag{A1}$$

with $0<\beta<1$.

The impact of degradation on the concentration profile can be established by scaling considerations. Morphogens in our model have a probability p of degradation at the end of each transition, hence the average number of transitions until degradation is $1/p$. The time t_{deg} beyond which degradation determines the length scale of the profile corresponds to the time at which $\langle n\rangle_{(t_{\mathrm{deg}})}=1/p$. By using the scaling law in Eq. (A1) we find that for anomalous diffusion $\lambda_\beta t_{\mathrm{deg}}^{\beta}=1$, with a generalized degradation coefficient $\lambda_\beta=p/\tau^{\beta}$.

The average distance a single morphogen particle traverses, and hence the length scale of the profile is proportional to $l\sqrt{\langle n\rangle}$, as for any random walk with transition length l. Therefore, below $\lambda_\beta t_{\mathrm{deg}}^{\beta}\ll 1$ the length scale of the profile will be time dependent [Eq. (A1)] and will behave similar to $\sqrt{D_\beta t^{\beta}}$ with a generalized diffusion coefficient $D_\beta=l^2/2\tau^{\beta}$. However, beyond $\lambda_\beta t_{\mathrm{deg}}^{\beta}\gg 1$ the number of transitions cannot exceed $1/p$, and the length scale of the profile will scale like $\sqrt{l^2/p}$. These results are consistent with the analytical solution for the two time regimes discussed in Sec. III B of the main text.

APPENDIX B: ANALYSIS OF A SHARP CHANGE IN THE TRANSITION TIME DISTRIBUTION

When the transition time distribution changes abruptly between two regions of space a discontinuity may form on the boundary between two regions. The notion of such discontinuities in the concentration profile is described in the literature for Fickian diffusion [51,52], and is attributed to chemical equilibrium on the interface. This concept of "chemical equilibrium" is obscure when applied to random walks, but it provides insight into why a discontinuity develops at the interface [53]. At equilibrium, the quantity of particles that move from region 1 to region 2 must equal the quantity leaving region 2 to region 1 (the net flux should be zero). If the characteristic transition length in the two regions is l_1 and l_2, then the quantity of particles that leave from region 1 to region 2 per unit area scales such as $l_1 C_1(x_{\mathrm{th}})\langle n_1\rangle_{(t)}$, where $\langle n_1\rangle_{(t)}$ is the average number of movements (transitions) after time t, and x_{th} is the position of the boundary between regions 1 and 2. The expression for the quantity of particles that leave from region 2 to region 1 is similar with a change of subscripts. From the equilibrium of local fluxes, and by using the scaling relation for $\langle n\rangle_{(t)}$ in Eq. (15) of the main text we obtain

$$\frac{l_1}{\tau_1^{\beta_1}} t^{\beta_1} C_1(x_{\mathrm{th}}) = \frac{l_2}{\tau_2^{\beta_2}} t^{\beta_2} C_2(x_{\mathrm{th}}). \tag{B1}$$

From Eq. (B1) we see that if the ratio $l_1/\tau_1^{\beta_1}$ and $l_2/\tau_2^{\beta_2}$ is not preserved, or when β varies between the two regions then a discontinuity in the concentration will arise. Notably, this discontinuity is still possible even as $\beta\to 1$ and the diffusion becomes Fickian.

A more mathematically rigorous boundary condition can be formalized using CTRW. It is be derived from the continuous space limit of Eq. (12) in Ref. [54]:

$$\tilde{C}(x,u) = \begin{cases} \tilde{R}(x,u)[1-\tilde{\psi}_1(u)]/u, & x\in(1), \\ \tilde{R}(x,u)[1-\tilde{\psi}_2(u)]/u, & x\in(2). \end{cases} \tag{B2}$$

Here, $R(x,t)$ is defined as the probability density function for a morphogen to "just arrive" at position x at time t, and subscripts (1) and (2) denote the two regions. We assume that the transition length distribution is the same in all regions of space, and therefore take $\tilde{R}(x,u)$ to be continuous at the boundary. Under this assumption Eq. (B2) leads to the boundary condition

$$\frac{\tilde{C}_1(x_{\rm th},u)}{\tilde{C}_2(x_{\rm th},u)} = \frac{1-\tilde{\psi}_1(u)}{1-\tilde{\psi}_2(u)}. \tag{B3}$$

In Sec. V of Ref. [57] we use this boundary condition and the partial differential form of CTRW [55] to derive a complete mathematical description of a region (clone) with different HSPG properties.

APPENDIX C: RECOVERY OF A BLEACHED REGION

In a FRAP experiment the recovery of fluorescence inside a photobleached region is measured as a function of time. The normalized intensity inside the photobleached region should increase as the square root of time for short times [47]. However, random walk simulations show that when the diffusion is anomalous, the intensity rises with time as a power law with an exponent of $1-\beta/2$ (main text). Here we demonstrate why an exponent larger than $1/2$ arises and investigate in Section VII of Ref. [57] a simple model problem for a recovery experiment.

The problem of recovery deals with the movement of morphogens that have been in the system for times that are of the order of the bleaching time t_b. It follows from scaling considerations that such morphogens are not equivalent to newly synthesized morphogens. If we denote the number of transitions of a morphogen from $t=0$ up to some time point t, by $\langle n\rangle_{(t)}$, then the number of transitions from t_b over the same time period t is $\langle n\rangle_{(t+t_b)}-\langle n\rangle_{(t_b)}$. It follows immediately from the scaling relation in Eq. (15) of the main text that the only case where $\langle n\rangle_{(t+t_b)}-\langle n\rangle_{(t_b)}=\langle n\rangle_{(t)}$ is when the diffusion is Fickian. Therefore, the transitions of newly synthesized morphogens are different from those that have stayed in the system for time t_b.

To investigate the system of such "aged" morphogens, we used results from aging continuous time random walks (ACTRW [49]). The ACTRW study shows that long after the onset of diffusion, morphogen population can be divided into two fractions: morphogens that are ready to perform new transitions, and morphogens that are still in the middle of a very long transition period and therefore are not free to diffuse (Fig. 5).

The fraction of morphogens that are free to move p_m depends on the bleaching time t_b and on the time that passed since the bleaching t. The double Laplace transform of p_m is [49]

$$\tilde{\tilde{p}}_m(s,u) = \frac{1}{u[1-\tilde{\psi}(s)]}\frac{\tilde{\psi}(s)-\tilde{\psi}(u)}{u-s}, \tag{C1}$$

where the tilde denotes the Laplace transformed function, u is the Laplace variable replacing t, and s is a second Laplace variable that replaces t_b. $\tilde{\psi}(u)$ and $\tilde{\psi}(s)$ are the Laplace transforms of the transition time distributions. When the diffusion is anomalous the transition probabilities have the asymptotic forms [49]

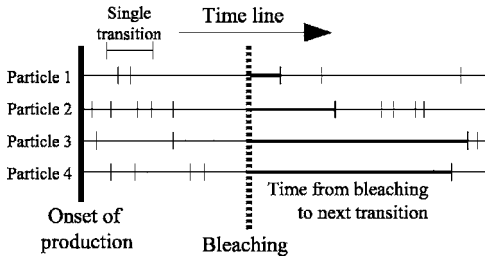

FIG. 5. Scheme of transition times after bleaching. Vertical lines denote the time-line in the life of a single morphogen particle and horizontal lines denote the end of a transition. Most morphogens at the bleaching time point (thick dashed line) are in the middle of a long transition. This fraction of morphogens can be visualized as a "store" that "releases" particles gradually with time. The "release" time is the horizontal thick line.

$$\tilde{\psi}(u) \approx 1-u^{\beta} \tag{C2a}$$

and

$$\tilde{\psi}(s) \approx 1-s^{\beta}. \tag{C2b}$$

We assume also that the time period after bleaching is much smaller than the time the morphogens spent in the system until the bleaching. Hence $t \ll t_b$ and $u \gg s$. Under this assumption, and with the use of the approximations (C2a) and (C2b), Eq. (C1) simplifies to

$$\tilde{\tilde{p}}_m(s,u) = \frac{1}{u^{2-\beta}s^{\beta}}. \tag{C3}$$

The inverse Laplace transform of Eq. (C3) is

$$p_m(t_b,t) = \frac{1}{\Gamma(2-\beta)\Gamma(\beta)}\left(\frac{t}{t_b}\right)^{1-\beta}. \tag{C4}$$

We see from Eq. (C4) that the fraction of morphogens that can diffuse increases in time as a power law. This time-dependent increase is the reason for the increase in the recovery exponent. However, despite having a larger power law exponent, recovery under conditions of anomalous diffusion is slower than recovery in the case of Fickian diffusion: whereas all morphogens are free to diffuse in Fickian diffusion, the fraction of free morphogens is very small under anomalous diffusion conditions.

[1] T. Tabata and Y. Takei, Development **131**, 703 (2004).
[2] J.-P. Vincent and L. Dubois, Dev. Cell **3**, 615 (2002).
[3] G.-H. Baeg, E. M. Selva, R. M. Goodman, R. Dasgupta, and N. Perrimon, Dev. Biol. **276**, 89 (2004).
[4] T. Y. Belenkaya, C. Han, D. Yan, R. J. Opoka, M. Khodoun, H. Liu, and X. Lin, Cell **119**, 231 (2004).
[5] C. Han, T. Y. Belenkaya, B. Wang, and X. Lin, Development **131**, 601 (2004).

[6] C. Han, T. Y. Belenkaya, M. Khodoun, M. Tauchi, X. Lin, and X. Lin, Development **131**, 1563 (2004).
[7] C. A. Kirkpatrick, B. D. Dimitroff, J. M. Rawson, and S. B. Selleck, Dev. Cell **7**, 513 (2004).
[8] J. Kreuger, L. Perez, A. J. Giraldez, and S. M. Cohen, Dev. Cell **7**, 503 (2004).
[9] K. Nybakken and N. Perrimon, Biochim. Biophys. Acta **1573**, 280 (2002).
[10] E. V. Entchev, A. Schwabedissen, and M. González-Gaitán, Cell **103**, 981 (2000).
[11] T. Bollenbach, K. Kruse, P. Pantazis, M. González-Gaitán, and F. Jülicher, Phys. Rev. Lett. **94**, 018103 (2005).
[12] A. Eldar, D. Rosin, B.-Z. Shilo, and N. Barkai, Dev. Cell **5**, 635 (2003).
[13] K. Kruse, P. Pantazis, T. Bollenbach, F. Jülicher, and M. González-Gaitán, Development **131**, 4843 (2004).
[14] A. D. Lander, Q. Nie, and F. Y. Wan, Dev. Cell **2**, 785 (2002).
[15] E. Muller-Horsche, D. Haarer, and H. Scher, Phys. Rev. B **35**, 1273 (1987).
[16] Q. Gu, E. A. Schiff, S. Grebner, F. Wang, and R. Schwarz, Phys. Rev. Lett. **76**, 3196 (1996).
[17] M. T. Cicerone, F. R. Blackburn, and M. D. Ediger, Macromolecules **28**, 8224 (1995).
[18] H. Weber and R. Kimmich, Macromolecules **26**, 2597 (1993).
[19] A. A. Gusev and U. W. Suter, J. Chem. Phys. **99**, 2228 (1993).
[20] O. Cardoso, B. Gluckmann, O. Parcollet, and P. Tabeling, Phys. Fluids **8**, 209 (1996).
[21] G. Kosakowski, B. Berkowitz, and H. Scher, J. Contam. Hydrol. **47**, 29 (2001).
[22] M. Levy and B. Berkowitz, J. Contam. Hydrol. **64**, 203 (2003).
[23] R. J. Cherry, P. R. Smith, I. E. G. Morrison, and N. Fernandez, FEBS Lett. **430**, 88 (1998).
[24] K. Ritchie, R. Iino, T. Fujiwara, K. Murase, and A. Kusumi, Mol. Membr Biol. **20**, 13 (2003).
[25] A. Caspi, R. Granek, and M. Elbaum, Phys. Rev. E **66**, 011916 (2002).
[26] I. Y. Wong, M. L. Gardel, D. R. Reichman, E. R. Weeks, M. T. Valentine, A. R. Bausch, and D. A. Weitz, Phys. Rev. Lett. **92**, 178101 (2004).
[27] A. S. Verkman, Trends Biochem. Sci. **27**, 27 (2002).
[28] H. Scher and M. Lax, Phys. Rev. B **7**, 4491 (1973).
[29] H. Scher and E. W. Montroll, Phys. Rev. B **12**, 2455 (1975).
[30] G. Pfister and H. Scher, Adv. Phys. **27**, 747 (1978).
[31] M. F. Shlesinger, J. Stat. Phys. **10**, 421 (1974).
[32] G. Margolin (private communication).
[33] R. Metzler and J. Klafter, Phys. Rep. **339**, 1 (2000).
[34] M. Fujise, S. Takeo, K. Kamimura, T. Matsuo, T. Aigaki, S. Izumi, and H. Nakato, Development **130**, 1515 (2003).
[35] X. Ai, A. T. Do, O. Lozynska, M. Kusche-Gullberg, U. Lindahl, and C. P. Emerson, Jr., J. Cell Biol. **162**, 341 (2003).
[36] G. K. Dhoot, M. K. Gustafsson, X. Ai, W. Sun, D. M. Standiford, and C. P. Emerson, Jr., Science **293**, 1663 (2001).
[37] O. Gerlitz and K. Basler, Genes Dev. **16**, 1055 (2002).
[38] A. J. Giráldez, R. R. Copley, and S. M. Cohen, Dev. Cell **2**, 667 (2002).
[39] G.-H. Baeg, X. Lin, N. Khare, S. Baumgartner, and N. Perrimon, Development **128**, 87 (2001).
[40] M. Strigini and S. M. Cohen, Curr. Biol. **10**, 293 (2000).
[41] A. A. Teleman and S. M. Cohen, Cell **103**, 971 (2000).
[42] J. Lippincott-Schwartz, E. Snapp, and A. Kenworthy, Nat. Rev. Mol. Cell Biol. **2**, 444 (2001).
[43] G. Carrero, D. McDonald, E. Crawford, G. de Vries, and M. J. Hendzel, Methods **29**, 14 (2003).
[44] N. Periasamy and A. S. Verkman, Biophys. J. **75**, 557 (1998).
[45] T. Feder, I. Brust-Mascher, J. P. Slattery, B. Baird, and W. W. Webb, Biophys. J. **70**, 2767 (1996).
[46] G. Georgiou, S. S. Bahra, A. R. Mackie, C. A. Wolfe, P. OShea, S. Ladha, N. Fernandez, and R. J. Cherry, Biophys. J. **82**, 1828 (2002).
[47] D. M. Soumpasis, Biophys. J. **41**, 95 (1983).
[48] M. J. Saxton, Biophys. J. **81**, 2226 (2001).
[49] E. Barkai and Y.-C. Cheng, J. Chem. Phys. **118**, 6167 (2003).
[50] D. J. Bornemann, J. E. Duncan, W. Staatz, S. Selleck, and R. Warrior, Development **131**, 1927 (2004).
[51] J. Crank, *The Mathematics of Diffusion*, 1st ed. (Oxford University Press, 1956).
[52] W. Jost, *Diffusion in Solids, Liquids, Gases*, 3rd printing ed. (Academic Press, 1960).
[53] A. Eldar (private communication).
[54] H. Scher and S. Rackovsky, J. Chem. Phys. **81**, 1994 (1984).
[55] A. Cortis, C. Gallo, H. Scher, and B. Berkowitz, Water Resour. Res. **40**, W04209 (2004).
[56] K. J. Hollenbeck, http://www.mathtools.net/files/net/invlap.zip (1998).
[57] See EPAPS Document No. E-PLEEE8-72-051510 for additional mathematical details and derivations. A direct link to this document may be found in the online article's HTML reference section. The document may also be reached via the EPAPS homepage (http://www.aip.org/pubservs/epaps.html) or from ftp.aip.org in the directory /epaps/. See the EPAPS homepage for more information.